A laboratory study of the retarding effects of braking mounds on snow avalanches

Kristín Martha HÁKONARDÓTTIR,[1] Andrew J. HOGG,[2] Tómas JÓHANNESSON,[1]
Gunnar G. TÓMASSON[3]

[1]*Icelandic Meteorological Office, Bústaðavegi 9, IS-150 Reykjavík, Iceland*
E-mail: tj@vedur.is
[2]*Centre for Environmental and Geophysical Flows, School of Mathematics, University of Bristol, University Walk, Bristol BS8 1TW, England*
[3]*VST Consulting Engineers, Ármúli 4, IS-108 Reykjavík, Iceland*

ABSTRACT. A series of laboratory experiments in a 6 m long chute using glass particles of mean diameter 100 μm were performed to investigate the interaction of a supercritical, granular flow with obstacles. It was found that the collision of the flow with a row of mounds led to the formation of a jet, whereby a large fraction of the flow was launched from the top of the mounds and subsequently landed back on the chute. The retarding effect of the mounds was investigated quantitatively by direct measurements of the velocity of the flow, its runout length and the geometry of the jet. The effects of several aspects of the layout of the mounds on their retarding effects were examined. It was observed that a row of steep mounds with an elongated shape in the transverse direction to the flow and with a height several times the flow depth led to dissipation of a large proportion of the kinetic energy of the flow.

1. INTRODUCTION

A system of avalanche protection measures has recently been constructed to defend part of the town Neskaupstaður in eastern Iceland (Fig. 1) (Tómasson and others, 1998a, b). The protection measures combine the use of snow-supporting structures in the avalanche starting zone, with two rows of "braking" mounds in the upper part of the runout zone, and a "catching" dam located just above the settlement to finally stop the avalanches. The main purpose of the braking mounds is to slow down the avalanche before it hits the dam so that the height of the dam can be reduced. In the preliminary design of the defence structures, it was assumed that after colliding with a row of mounds, an avalanche would slow down by approximately 20%. In the absence of design guidelines for braking mounds, this was based on an extrapolation of avalanche design guidelines from Switzerland (Voellmy, 1955; Salm, 1987) and on design methods and experimental observations for energy dissipators in hydraulic stilling basins and spillways. At later stages of the design, small-scale laboratory experiments with high-speed granular flows hitting obstacles were conducted. The goal of these experiments was to find an optimum layout and geometry of braking mounds and to obtain an estimate of the energy dissipation. In this context, the terms "dissipation" or "granular dissipation" are used to denote a reduction of the mechanical energy of the avalanche that is brought about by the interaction between the granular flow and the mounds.

Despite the absence of accepted guidelines for the design of braking mounds for retarding snow avalanches, mounds are widely used for protection against dense, wet-snow avalanches, although they are thought by some to have little effect against dry, rapidly moving snow avalanches (see,

e.g., McClung and Schaerer, 1993; Norem, 1994). Salm (1987), on the other hand, has formulated an estimate for the reduction in the speed of an avalanche that hits several obstacles, such as buildings, that are spread over the runout area of the avalanche and assumed to cover a certain fraction, c, of the cross-sectional area of the flow path. According to this expression, the speed of the avalanche is reduced by the ratio $c/2$, assuming that the obstacles are sufficiently strong and are not swept away by the avalanche. The expression indicates a substantial effect of the obstructions on the speed of the avalanche. Voellmy (1955) proposes a similar

Fig. 1. A photograph of the braking mounds in Neskaupstaður and the catching dam behind them. Each mound is 10 m high, and the catching dam 17 m high.

191

expression for the reduction in the speed of an avalanche that hits several rows of trees. These expressions are not derived from a conceptual model of the flow around obstacles and it is not clear whether they may be expected to apply to a rapidly moving, dry-snow avalanche.

Braking mounds designed to retard rapidly moving dry-snow avalanches will in most cases be of a height that is only a small fraction of the height scale corresponding to the kinetic energy of the avalanche, which is defined by $u^2/2g$, where u is the speed of the flow and g is the gravitational acceleration. One might expect that having flowed up the mounds, the avalanche could regain some of the kinetic energy spent when it descends along the backside of the mounds. Salm's expression nevertheless suggests that the kinetic energy of the avalanche is reduced by 44% by one row of mounds covering 50% of the cross-sectional area of the path, and Voellmy's expression leads to a similar conclusion. The energy dissipation must, if the mounds are in fact as effective as they assume, be brought about by irregularities and mixing introduced by the abrupt deviation of the avalanche flow over and around the mounds. Such an effect may be expected to depend to a high degree on various details in the layout and geometry of the mounds, making the lack of established guidelines for the design of avalanche mounds particularly acute. One may also note that the volume of the avalanche will typically be so large that only a small fraction of the snow near the front of the avalanche is needed to fill the space upstream of the mounds so that they become effectively buried and the bulk of the avalanche easily overflows the mounds. For the braking mounds to be effective while the avalanche passes over them, they must not become buried by the avalanche.

Laboratory-scale experiments with granular flows have been carried out by a number of investigators (e.g. Savage and Hutter, 1989; Johnson and others, 1990; Hutter and others, 1995; Wieland and others, 1999). These studies have used laboratory investigations to illuminate phenomena which occur in granular flows and to validate theoretical models. There remain a number of unresolved issues using laboratory-scale experiments to understand natural-scale phenomena because in contrast to purely fluid flow, it remains unclear how to maintain dynamical similarity. In contrast to many of the previous investigations, we focus on motion at high Froude numbers and analyze the interaction with solid obstacles placed in the flow. In this context, we define the Froude number in terms of the flow velocity, the gravitational acceleration and the flow depth, h, by:

$$\mathrm{Fr} = \frac{u}{\sqrt{gh}}. \tag{1}$$

It is a dimensionless number which is used to describe free-surface fluid flow, and represents the ratio of the kinetic energy of the flow to the internal potential energy, or the ratio of the flow velocity to the speed of long-wavelength free-surface gravity waves in the flow.

Laboratory experiments have previously been performed to investigate granular flows hitting catching dams (Chu and others, 1995) and deflecting dams (Tai and others, 2001), but we are not aware of previous experiments with retarding structures such as braking mounds. The design of the experiments reported here was based on the conjecture that if the Froude numbers were of the same order of magnitude, dynamical similarity between natural snow avalanches and the smaller-scale experimental avalanches would be maintained.
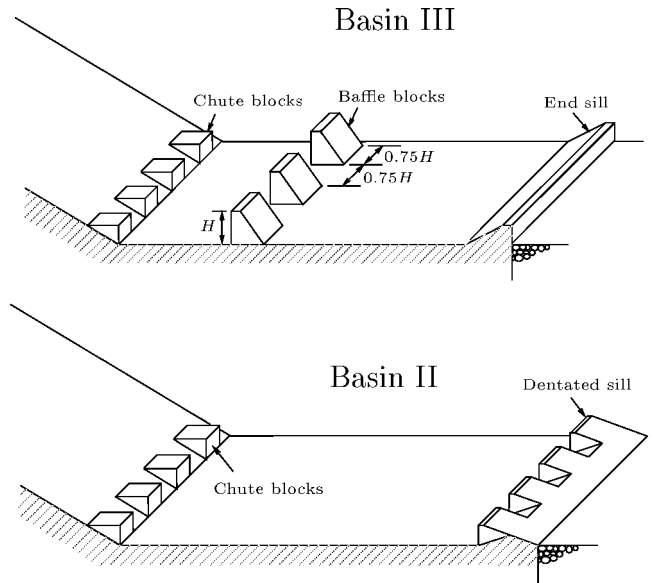

Fig. 2. Baffle blocks and other energy dissipators used in waterways when $\mathrm{Fr} > 4.5$ *(see USBR, 1987, for a description of the retarding effect of these structures on fluid flow).*

An insignificant retardation at the laboratory scale would suggest that this effect would also be small for natural snow avalanches. On the other hand, a result indicating a substantial retardation would not necessarily apply to natural avalanches due to the different physics of the flows, such as compression of the snow in the impact with the mounds, different frictional properties of the materials and the effect of air resistance on the jet that arises during the interaction with the mounds. Nevertheless we believe we have identified certain types of behaviour which do not strongly depend on scale or material properties and which may be exploited in the design of avalanche protection measures in Neskaupstaður or other locations. In this paper, we report on the experimental investigations carried out at the Centre for Environmental and Geophysical Flows, University of Bristol (Woods and Hogg, 1998, 1999; Hákonardóttir, 2000).

Braking mounds have been studied previously in the context of fluid flows (Peterka, 1984; USBR, 1987; Hager, 1995; Roberson and others, 1997). The corresponding structures are called baffle blocks and are commonly used as energy dissipators in hydraulic waterways (Fig. 2). The scale of the flow in these structures is often more than an order of magnitude larger than in the laboratory experiments described here, with flow speeds up to $30–40\,\mathrm{m\,s^{-1}}$ which are similar to the speeds of natural avalanches (McClung and Schaerer, 1993). Some experiments with energy dissipators in waterways show jets launched from braking mounds that are similar to the jets observed in the current experiments (Gerodetti, 1985).

In this paper, we first present the laboratory set-up for the experiments where interaction of high-speed granular currents with a row of obstacles is studied (section 2). We move on to report on the experimental results in section 3, first by looking at the flow of a granular current down the experimental chute without any obstacles present (section 3.1). Then the results of experiments using obstacles with different shapes and sizes are stated and their retarding effects compared (section 3.2). We conclude with a summary of the experimental results (section 4).
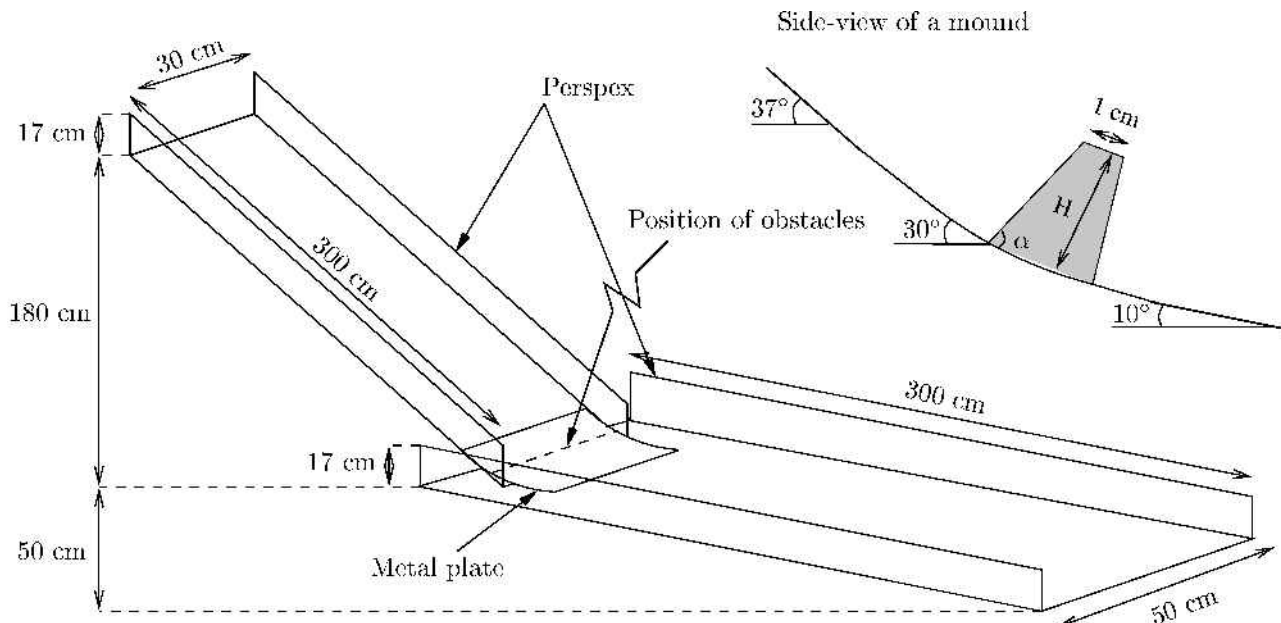
Fig. 3. Schematic diagram of the chute, and a side-view of a mound positioned on the experimental chute.

2. EXPERIMENTAL SET-UP

2.1. Design

The laboratory experiments were designed to quantify the retarding effect of braking mounds on high-Froude-number granular flows down an inclined chute. Barriers were placed across the chute in a row perpendicular to the axis of the chute. Experiments using one row of barriers were compared with a control experiment in which no obstacles were used.

The experiments were designed so that the current of particles had a high internal Froude number, close to that of a natural snow avalanche. A typical value for the speed of a dry-snow avalanche is $30–50\,\mathrm{m\,s^{-1}}$, and the depth of the dense part is $1–3\,\mathrm{m}$, leading to a Froude number of order 10. The speed of propagation of disturbances (small-amplitude surface waves) in high-Froude-number flow is less than the flow speed. Thus, the flow upstream of a barrier can be assumed to be undisturbed by the presence of the barrier.

The model barriers were designed so that the ratio of the height of the barriers to the flow depth was $1–7$. The barrier Froude number is defined in terms of the flow velocity and the height of the barriers, H, as

$$\mathrm{Fr_b} = \frac{u}{\sqrt{gH}}\,, \qquad (2)$$

and represents the ratio of the kinetic energy of the current to the potential energy corresponding to the height of the barriers. It is an important parameter for characterizing the interaction of the flow with the barriers. The barrier Froude number in the experiments was in the range $3 < \mathrm{Fr_b} < 9$.

2.2. Experimental apparatus

The experiments were performed on a 6 m long wooden chute consisting of two straight sections. They were connected by a curved metal sheet to allow for a smooth transition between the two sections of the chute. A row of obstacles was located at the end of the upper chute, 2.7 m downslope from where the flow was released. At that point the metal plate was inclined at $30°$. The barriers were con-

structed of a rigid plastic material with heights, H, between 1 and 7 cm and angles between the upstream face of the mounds and the chute, α, in the range $30–90°$ (Fig. 3).

Glass beads (ballotini) of mean size $100\,\mu\mathrm{m}$, density 2500 $\mathrm{kg\,m^{-3}}$ and an approximately spherical shape were used in the experiments. The granular material had a bulk density of $1600\,\mathrm{kg\,m^{-3}}$, an angle of repose of $25–26°$ and a dynamic bed friction angle close to $22°$. The coefficient of restitution was measured to be 0.8 for $350\,\mu\mathrm{m}$ ballotini and may be expected to be similar for the $100\,\mu\mathrm{m}$ ballotini used in the experiments.

2.3. Experimental technique

In each experiment a measured quantity of particles was released instantaneously from the top of the chute. The motion down the slope was recorded by video and subsequently analyzed, and the runout length and distribution of the deposited particles were measured.

In order to simplify the presentation of the experimental results, a datum configuration of the mound geometry and avalanche size was selected. The datum configuration consisted of a mass released of 6 kg and three elongated mounds covering 60% of the width of the chute. The mounds had their upstream face perpendicular to the chute, a height of 3 cm (approximately 3 times the flow depth) and a width of 6 cm (Fig. 4).

The Froude number for these experiments was measured in the following way. First the speed was determined by analysis of video footage of the grain flow down the slope. Both the front speed and interior speed were measured, the latter being determined by tracking tracer particles in the flow. Two video cameras were used to film the experiments, operating at 50 and 500 frames per second. For the datum flow configuration, flow speeds in the range $2.8 \pm 0.1\,\mathrm{m\,s^{-1}}$ were measured for the interior of the flow just above the mounds. The depth of the flow was measured by inserting a horizontal plate over the chute and adjusting its height until the current flowed under it. The flow depth just above
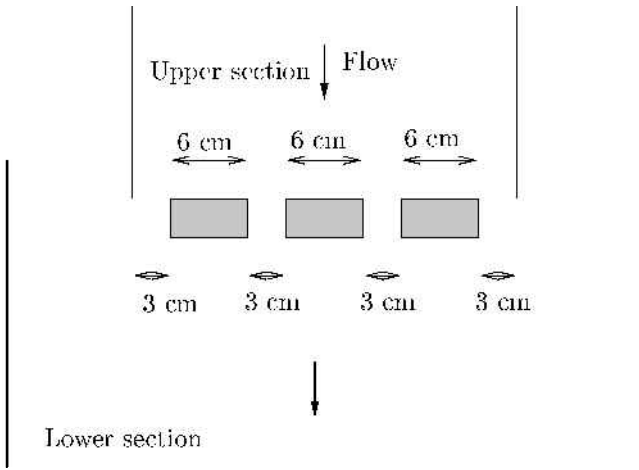
193

Fig. 4. Datum configuration of the mound geometry, plan view.

the mounds was 1.0 ± 0.05 cm. Thus the Froude number for the datum experiments was approximately 9.

Experiments were carried out in order to analyze the oncoming flow at the mounds, and then to investigate the retarding effects of mounds by systematically changing their layout and geometry and comparing the results to those obtained for flow over a dam and to a control experiment without any obstacles in the flow path. Two series of experiments were conducted: (1) an analysis of the flow on the upper section of the chute in which the mass of the granular avalanche was varied, and (2) an investigation of the interaction of the flow with the braking mounds in which the following changes in the layout of the mounds were made.

The aspect ratio, H/B, of the mounds was varied, where H is the mound height and B the breadth, while the angle between the upstream face of the mound and the

chute, α, and the proportion of the width of the chute covered by mounds, A_m/A_{tot}, were kept fixed; here A_{tot} is the width of the chute and A_m denotes the width that the mounds cover.

The relative height of the mounds to the flow depth, H/h, was varied while the upstream angle α, the proportion of the width of the chute blocked by mounds, A_m/A_{tot}, and the breadth of the mounds, B, were held constant.

The mound spacing and layout was studied by keeping the aspect ratio, H/B, the relative height, H/h, and upstream angle, α, fixed as the mound spacing was changed for different proportions of the chute blocked by mounds, A_m/A_{tot}.

3. EXPERIMENTAL RESULTS

3.1. Flow without mounds

The control experiment consisted of releasing 6 kg of material down the experimental chute, without any obstacles present. The flow ran out to a distance $x_{cont} = 1.74 \pm 0.01$ m, measured from the junction of the lower section of the chute and the metal plate to the leading edge of the deposit. The experiment was repeated regularly throughout the experimental period, leading to consistent values of x_{cont}.

The granular current quickly reached a terminal speed of 3.6 ± 0.1 m s^{-1}, which remained constant until the slope angle changed close to the bottom of the upper chute. The flow started to decelerate on the metal plate, connecting the two segments of the chute, and by the time it reached the point where the mounds would later be placed, the speed was 2.8 ± 0.1 m s^{-1} and the flow thickness was 1.0 ± 0.05 cm. This corresponds to an internal Froude number of approximately 9. The flow came to rest, rather abruptly, on the lower section about 2 s after its release. The first flow front reached furthest, but particles in the internal part of the flow were observed to flow on top of material already at rest, forming a layered deposit.

The effect of varying the total mass of material released on the Froude number of the flow on the upper section of the chute was investigated. It was found that once the flow had reached its terminal speed on the upper section, the Froude number was approximately independent of the amount of material released. The terminal flow speed varied from about 3.1 ± 0.1 m s^{-1} for 3 kg of the material to about 3.6 ± 0.1 m s^{-1} for 8.5 kg, and the flow thickness from about 0.7 ± 0.05 cm for 3 kg to about 1.1 ± 0.05 cm for 8.5 kg, resulting in Froude numbers in the range $11-13$.

3.2. Flow with mounds

3.2.1. The jet formed by the collision with the mounds
It was observed that the collision of the flow with a row of mounds leads to the formation of a jump or a jet, whereby a large fraction of the flow is launched from the top of the mounds and subsequently lands back on the chute. The jet for the datum experiment (Fig. 4) was analyzed in some detail. As the first front of the stream hits an obstacle, particles are launched from the top of the obstacle at an angle close to its upstream angle, α. The jet rapidly adjusts to a new angle, henceforth termed the throw angle, which is less than α, and reaches a quasi-steady state as the bulk of the current
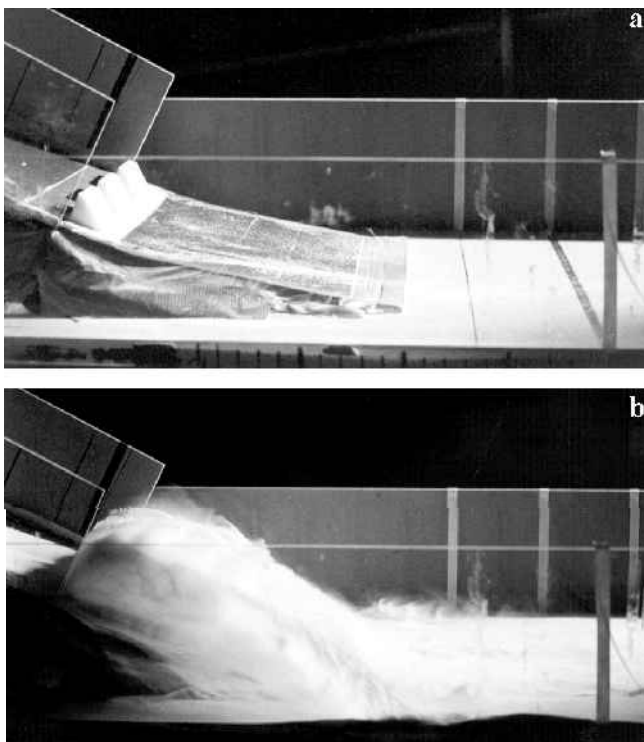

Fig. 5. Photographs of (a) the datum mound configuration and (b) jet in a quasi-steady state on the experimental chute.
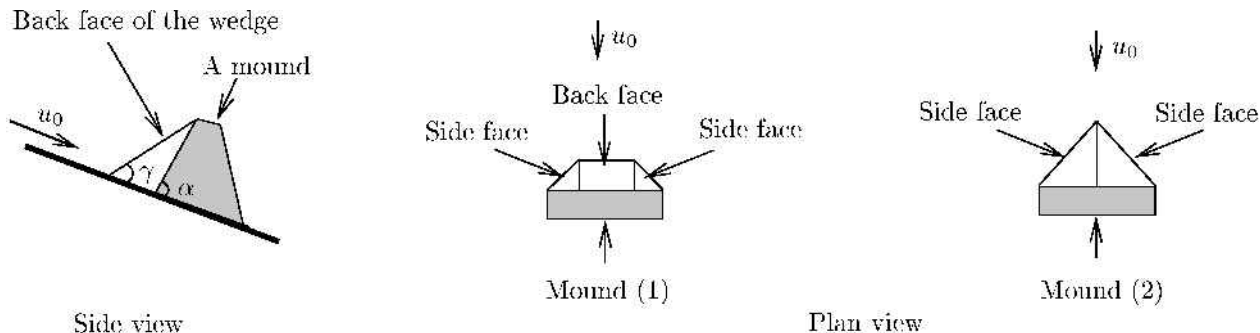
Fig. 6. A wedge formed behind a mound indicating the angle γ with respect to the chute. Also shown is the plan view of a wedge formed behind mounds with different aspect ratios: $H_1/B_1 < H_2/B_2$. For mound (1), the granular current jumps over the mound as well as being deflected around it. For mound (2), the side faces of the wedge have joined and none of the flow jumps over the mound.

passes over the barrier as a coherent jet (Fig. 5). This part of the jet lands furthest away from the mounds. After the main flow has passed over the mounds, the jet quickly dies out.

There is a considerable difference between the flow over a continuous dam and several separate barriers across the slope. Whereas the flow over a dam is essentially two-dimensional, the flow over and around a mound is three-dimensional, as the granular material is deflected both upwards and sidewards. A wedge of particles is formed behind the upstream face of the mound during the flow (Fig. 6). It was observed that the part of the stream that hits the back face of the wedge flows directly over the mound, but the part that hits the side faces is deflected in the plane of the side face (for a more detailed discussion, see section 3.2.2).

A first approach to model the jet of particles is to treat it as a projectile motion in two dimensions (Fig. 7). A balance of forces can be written as

$$\mathbf{F} = m\mathbf{g} - mk\dot{\mathbf{x}}|\dot{\mathbf{x}}|, \tag{3}$$

where $\mathbf{F}$ is the force exerted on the mass, m, $\mathbf{g}$ is the gravitational acceleration, k is a dimensional constant representing a turbulent drag caused by air resistance and $\mathbf{x} = (x, z)$ is the location of the particle in horizontal and vertical directions, respectively. The motion is subject to the initial conditions

$$z = x = 0 \qquad \text{at} \qquad t = 0 \tag{4}$$

and

$$\dot{x}(0) = u_1 \cos\theta, \tag{5}$$
$$\dot{z}(0) = u_1 \sin\theta, \tag{6}$$

where u_1 is the speed of the current when it is launched from the top of the obstacle at an angle, θ, relative to the horizontal (Fig. 7). It was found that the geometry of the jet at this laboratory scale was best modelled by neglecting air resis-
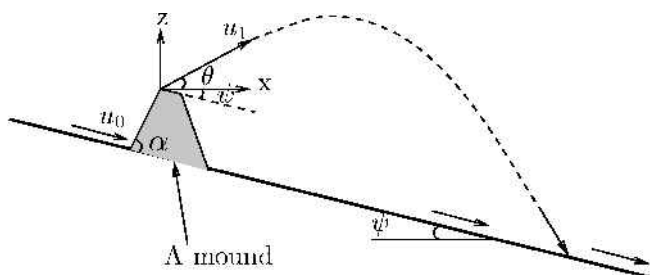
tance and thus setting the coefficient k equal to zero. This leads to an equation for the trajectory of the jump,

$$z = x \tan\theta - \frac{1}{2}\frac{gx^2}{u_1^2}\sec^2\theta. \tag{7}$$

The oncoming speed, u_0, was measured in each experiment along with the trajectory of the jet. The parameters that define the geometry of the steady jet are the throw
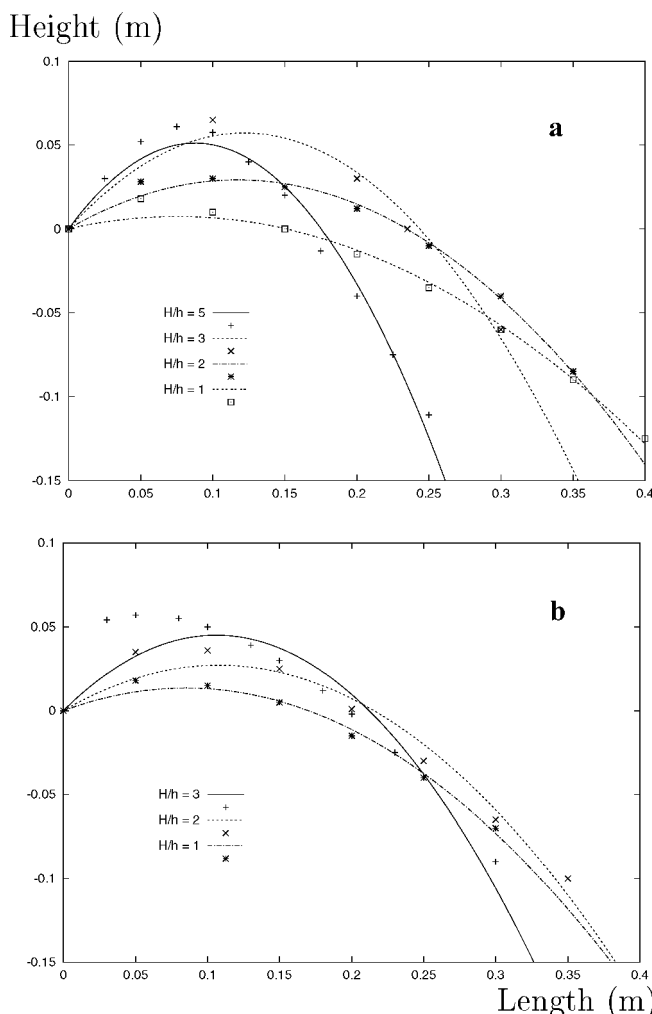
Height (m)

Length (m)

Fig. 8. (a) The jet profiles for flow over dams with $\alpha = 90°$ and varying heights. (b) The jet profiles for flow over the datum mound configuration with $\alpha = 90°$ and varying obstacle heights. The jets are plotted using the coordinate system defined by Figure 7. In each case, the curve shown is the best-fit parabola through the data points.
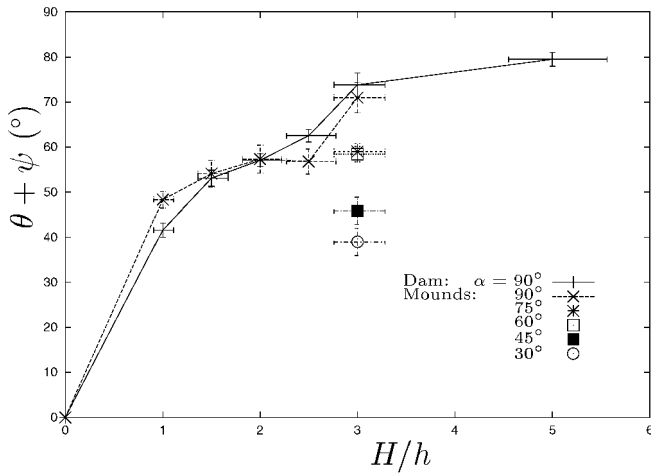

Fig. 7. Schematic diagram of a jet, side-view. The throw angle, θ, and the inclination of the chute, ψ, defined.

Fig. 9. The throw angle, $\theta + \psi$, plotted as a function of the non-dimensional height, H/h, for a dam ($+$) and a datum mound configuration ($\times$) with $\alpha = 90°$. The upstream angle of the mounds, α, is also varied for the datum mound configuration and $H/h = 3$.
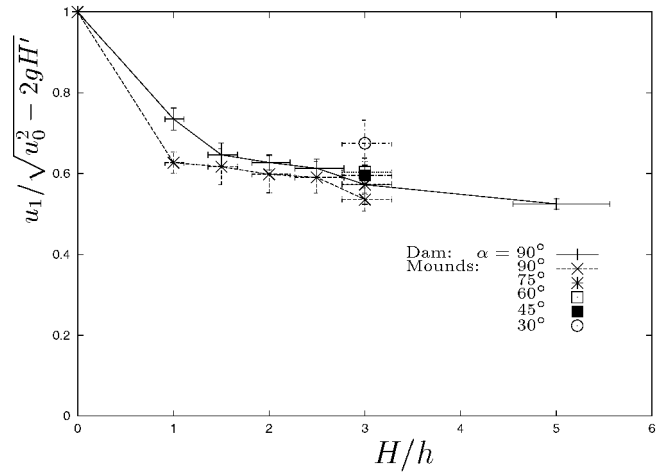

Fig. 10. The ratio $u_1/\sqrt{u_0^2 - 2gH'}$ plotted as a function of the non-dimensional height, H/h, for a dam ($+$) and the datum mound configuration ($\times$) with $\alpha = 90°$. The upstream angle of the mounds, α, is also varied for the datum mound configuration with $H/h = 3$.

angle, θ, and the velocity, u_1. It was hard to measure θ and u_1 directly from the video recordings since a cloud of particles obstructed a clear vision of the jet. They could nevertheless be calculated indirectly as follows. The trajectory of the jump was very well defined in the experiments; thus a parabola $z = ax - b^2x^2$ could be fitted to the trajectory using least-squares regression (Fig. 8). Hence,

$$\theta = \arctan a \,, \tag{8}$$

$$u_1 = \frac{\sec \theta}{b} \sqrt{\frac{g}{2}}. \tag{9}$$

Understanding of the factors that determine θ and u_1 is fundamental to be able to predict the trajectory of the jet. It was anticipated that the throw angle, θ, would be a function of the height of the barriers relative to the thickness of the oncoming stream, the internal Froude number of the flow and the angle of the upstream face of the mounds. In order to examine this dependence, $\theta + \psi$ (where $\psi = 30°$ is the inclination of the chute in which the mounds are positioned) was plotted as a function of the height of the mounds over the flow depth, H/h (Fig. 9). From Figure 9 it can be observed that $\theta + \psi$ increases to an angle close to α as the relative height of the dam increases. The situation is more complicated for the mounds because of the three-dimensionality of the flow. For the smaller mounds ($H/h \leq 3$), θ changes in the same way as for the dam. However when $H/h \geq 5$, the side faces of the wedge join and the material is deflected sideways in the plane of the faces rather than directly over the mounds. The flow has then become three-dimensional, so it is inappropriate to consider just the angle θ.

A considerable proportion of the energy is dissipated when the flow hits the mounds and lands again on the chute. If the mechanical energy of the flow is conserved in the initial collision with the mounds, simple energy conservation gives

$$\frac{1}{2} u_1^2 = \frac{1}{2} u_0^2 - gH' \,, \tag{10}$$

where H' is the vertical rise of the flow when it passes over the

obstacles ($H' = H \sin(\alpha - \psi)/\sin \alpha$). Hence, this gives the expression

$$\frac{u_1}{\sqrt{u_0^2 - 2gH'}} = 1 \,. \tag{11}$$

Plotting the ratio $u_1/\sqrt{u_0^2 - 2gH'}$ provides an estimate of the amount of energy dissipated in the turning process, since if kinetic energy is solely converted into gravitational potential energy, then this ratio should be unity. We plot this ratio (11) as a function of the obstacle height relative to the flow depth in Figure 10 for both flows over a dam and mounds in the datum configuration for which the inclination of the upstream face is varied. We observe that a substantial fraction of the energy is dissipated in the impact. The velocity is lowered by around 35% for a relative mound height of 1. Further increase in the mound height leads to further lowering of the velocity, and the velocity is reduced by about 40% for a non-dimensional mound height of 3. The experiments indicate that mounds and dams dissipate energy, measured in this way, by a similar amount during the initial impact. We note that in this calculation we have not accounted for any infill behind the obstacle, which could somewhat reduce the effective height of the obstacles, H', with the result that we may be slightly underestimating the energy loss.

There was no notable effect of air resistance on the geometry of the jets in the current experiments. This is not necessarily the case for natural snow avalanches where the flow speed of the jet is considerably higher, and the term $mk\dot{\mathbf{x}}|\dot{\mathbf{x}}|$ in Equation (3) could become significant. Full-scale experiments with water jets suggest that up to 30% of the initial kinetic energy of the jet could be lost during the airborne phase (see USBR, 1987; Novak and others, 1989; Hager, 1995). The dense core of an avalanche is approximately $200 \, \text{kg m}^{-3}$ (McClung and Schaerer, 1993) and so is less dense than water. Therefore, it is reasonable to conclude that the avalanche jet is affected by air resistance at least to the same extent as a jet of water, leading to a shortening of the trajectory of the jets compared to a jet that is not affected by air resistance.

The airborne jet that is formed by the collision of the flow with the mounds has important practical consequences for the use of multiple rows of mounds to retard avalanches. The
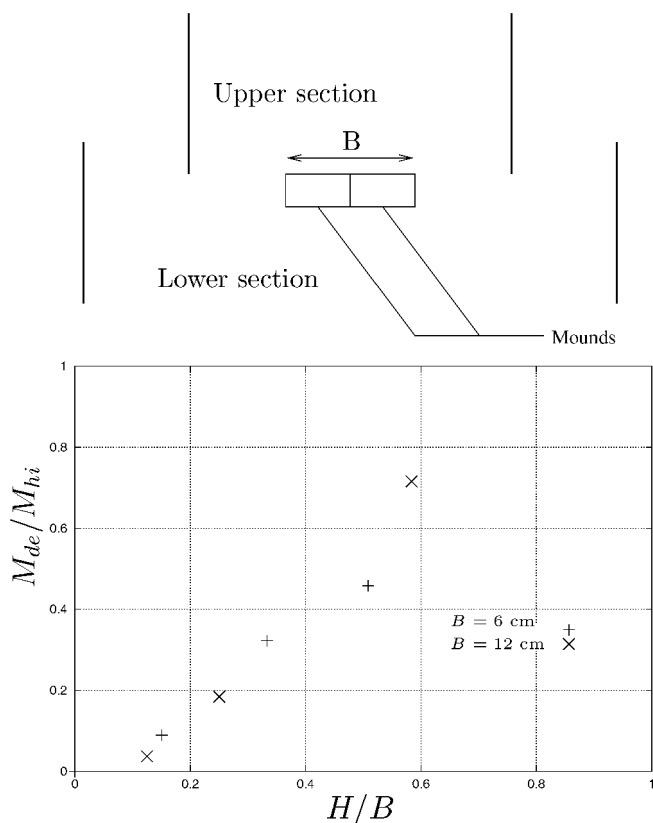
196

Fig. 11. The proportion of mass deflected, M_{de}, and mass hitting an obstacle, M_{hi}, (see plan view above) plotted as a function of the aspect ratio of the obstacle, H/B.

Fig. 12. The runout relative to the control, x/x_{cont}, as a function of the non-dimensional height of the obstacles, H/h, for a dam (+) and the datum mound set-up (×).

spacing between the rows must be chosen sufficiently long so that the material launched from the mounds does not jump over rows further down the slope in order for the lower rows to have full retarding effect. The spacing between the two rows of mounds in Neskaupstaður was determined based on computed trajectories for a jet launched from the first row in order to provide sufficient space for the material to land in front of the second row. It was assumed that energy lost due to air resistance was similar to the full-scale experiments with the high-speed water jets mentioned above.

3.2.2. The aspect ratio of the mounds, H/B

An experimental set-up of one obstacle positioned in the middle of the chute, was used and its aspect ratio varied (Fig. 11). It was anticipated that the ratio M_{de}/M_{hi}, where M_{de} is the mass that the obstacle deflects into the passing stream and M_{hi} is the mass heading for the obstacle, would be non-zero since some of the material is deflected laterally and would be a function of the aspect ratio of the mound.

In the initial impact a wedge was built up at the upstream face of the mound, and its shape was partly determined by the ratio of the height of the mound to the breadth, H/B. When the stream hits the "back face" of the wedge it flows directly over the mound, but when it hits the "side faces" it is deflected in their plane (see Fig. 6). When a mound becomes sufficiently high compared to its breadth, the side faces of the wedge join and all of the flow heading for the mound is deflected sideways rather than being launched from the top of the mound. Figure 11 reflects this process: when the height of the mounds is small compared to their breadth, only a small proportion of the mass heading for a mound is deflected away from it. As the height of the
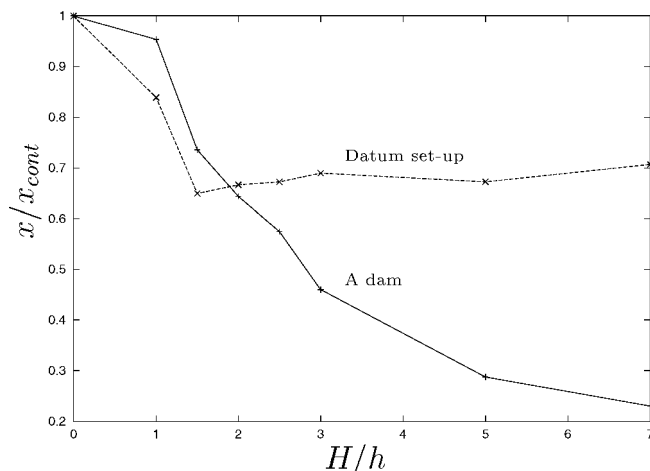
mounds is increased, a larger proportion of the flow is deflected from the mounds and finally, when the mounds have become high enough, the two side faces of the wedge join and none of the flow jumps over the obstacle. It should be noted that since the wedge is not formed instantaneously, there is always a part of the mass that is launched from the top of a mound, before the wedge is fully formed.

The way in which the interaction of the flow with mounds dissipates energy must depend in part on what proportion of the flow jumps over the mounds and what proportion is deflected sideways around them. Once the side faces of the wedge join and the flow ceases to jump over the mounds, their ability to dissipate energy, for a fixed mound configuration, has reached a limit, and increasing H further does not affect the way in which the flow is deflected from the mounds. The ratio H/B of the mounds is therefore critical in their design. The experiments suggest that the two side faces join when H/B is close to 0.8. In order to explain the data plotted in Figure 11, the angle between the back face of the wedge and the chute, γ, needs to be calculated, as well as the angle between the side faces of the wedge and the chute. Both angles might be expected to depend on the angle of repose of the material and γ to be highly dependent on the Froude number of the flow.

3.2.3. The relative height of the mounds, H/h

In a second series of experiments, the height of the obstacles was systematically varied while the upstream angle, α, was kept constant at $90°$ and the runout was measured for each experiment (Fig. 12). Obstacles in the chute were either a dam or a set of mounds in the datum configuration (see Fig. 4). For dams, the runout decreased monotonically as the height of the dam increased. Increasing the height of the mounds, on the other hand, had no effect on the runout length after H/h exceeded a value of approximately 2. It is worth noting that for the lower obstacles ($H/h \leq 2$), the datum configuration of the mounds leads to a shorter runout than that for a dam.

Parabolas were fitted to the measured trajectories of the quasi-steady jets launched from the top of the obstacles (see section 3.2.1). For the experiments with a dam, the measured jets were well described by a parabola. The jet trajectory for the lower mounds, $H/h < 5$, also had a parabolic shape (Fig. 8). However, for the higher mounds, $H/h \geq 5$, the bulk of the current was deflected sideways in the plane of the side

197

faces, rather than being launched from the top of the mounds.

3.2.4. Mound spacing and layout

In order to examine the way in which different mound configurations affect the runout of the flow, various configurations of 3 cm high and 6 cm wide mounds were employed. The mounds were positioned within the chute as shown in the plan view in Figure 13. The runout was recorded along with the mass of material jumping over the mounds, M_j, for various proportions of the cross-sectional area of the upper segment of the chute covered by mounds, A_m/A_{tot}. The amount of material jumping over the mounds was measured as before.

The experiments showed that the mounds were more effective at shortening the runout distance when a larger area of the chute was covered with mounds, and a continuous dam across the chute had the greatest retarding effect (Fig. 13a). The layout of the mounds covering the same total cross-sectional area also had some effect, such that having many small gaps led to the shortest runouts, i.e. configuration (5) was more effective than (4), and (7) and (8) were more effective than (6) (note in experiment (6) the aspect ratio of the mounds changes). Figure 13b confirms that a considerable amount of the flow heading for the mounds is deflected around them rather than being launched from their top. That is, the mass jumping over the mounds is not directly proportional to the proportion of the width of the chute covered by mounds ($M_j/M_{tot} < A_m/A_{tot}$).

By viewing the airborne jets from above, it was observed that the jet streams from the different mounds mixed. In the gap between any two mounds, two jets were deflected at each other, leading to repeated particle collisions in a narrow zone between the mounds, where particles bounced in and out of the main jet streams.

3.2.5. Slope of upstream mound faces

The effect of changing the upstream angle of the mounds, α, on the runout is plotted in Figure 14. Datum set-up (Fig. 4) was used in all experiments reported in this section. The mounds were situated on a slope of $30°$, hence, for example, an upstream face inclined at $45°$ corresponds to an inclination of $15°$ to the horizontal. It was observed that the runout decreased with increasing slope of the mound faces. For an angle $\alpha \leq 45°$ no wedge was formed at the upstream face of the mounds ($\alpha < \gamma$). An angle of $> 45°$ was found to lead to a greater decrease in runout length than a smaller angle. Increasing the angle further than about $60°$ did not lead to a substantial further decrease in runout.

4. CONCLUSIONS

Braking mounds seem to have a substantial retarding effect on high-Froude-number granular currents, similar to what is well established for baffle blocks which are used as energy dissipators in hydraulic structures. The experiments indicate that the effectiveness of the mounds depends on several aspects of their layout. Specifically examined in this study were the influence of the height of the mounds relative to the depth of the oncoming stream, H/h; the upstream angle between the mounds and the chute, α; the height of the mounds relative to their width, H/B; and the proportion of the width of the impact zone covered by the mounds, A_m/A_{tot}.

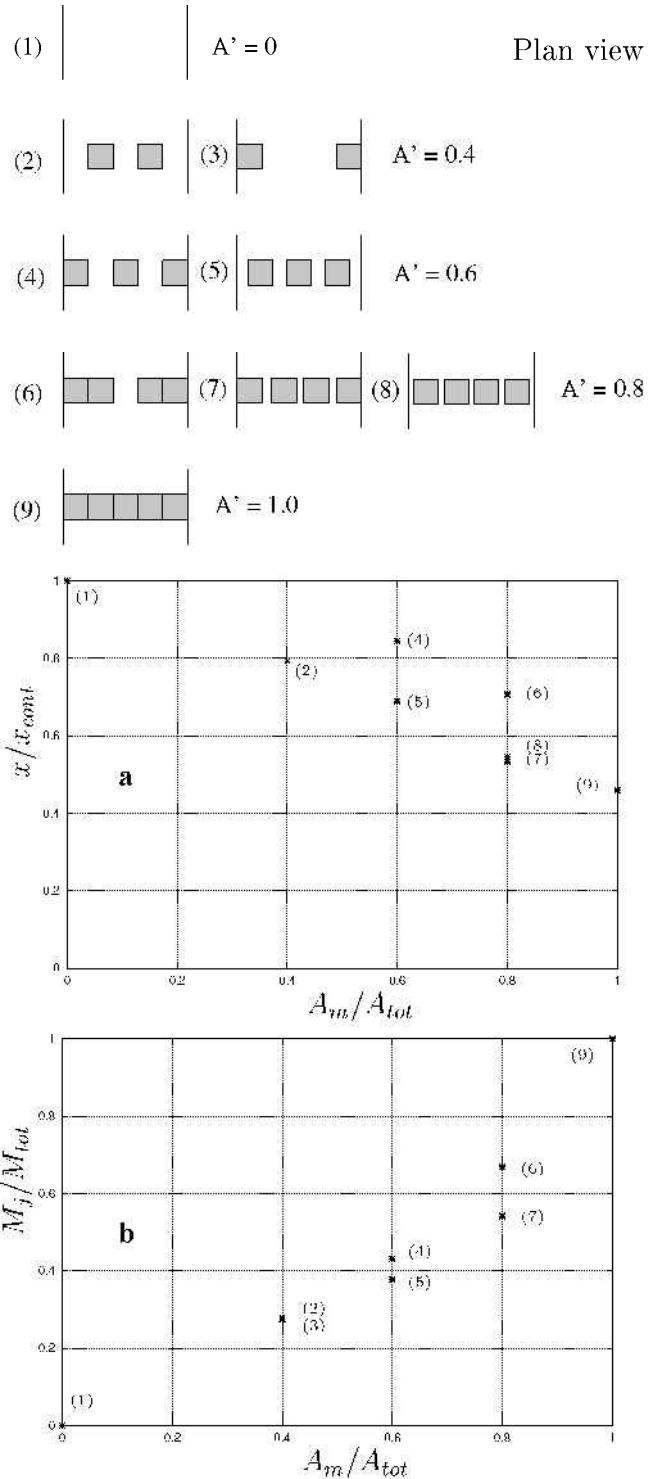The experiments indicate that energy is dissipated

Fig. 13. Effect of different mound configurations (see plan view) on (a) the runout of the material and (b) the mass of material jumping over the mounds. x/x_{cont} is the runout relative to the runout of the control experiment, M_j/M_{tot} is the mass of the flow jumping over the mounds relative to the total mass released, and $A' = A_m/A_{tot}$ is the proportion of the width of the chute covered by mounds. The runout was not measured for configuration (3) which henceforth does not appear on the first graph, and the mass jumping over the mounds was not measured for configuration (8) and is therefore not included on the second graph.

during the impact with the mounds, in the airborne jet flow and in the jet-landing as a result of mixing between streams flowing in different directions. When the aspect ratio of the mounds is small enough ($H/B < 0.8$), projectile motion can
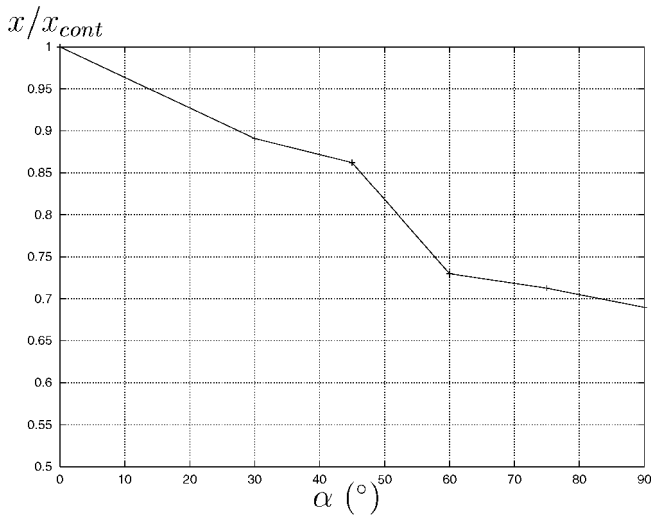
x/x_{cont}

Fig. 14. Non-dimensional runout, $x/x_{\rm cont}$ plotted as a function of the angle of the upstream face of the mounds, α.

be used to model the trajectory of material launched off the mounds. The angle and the velocity at which the material jumps off the mounds depend on the ratio of H/h and on the upstream angle of the mounds, α, along with γ, the angle of the wedge built up at the back face of the mounds. The energy dissipated by the mounds increases with the mound height until the aspect ratio reaches a certain value. This value corresponds to the joining of the two side faces of the wedge that is formed upstream of each mound. A further increase in the mound height does not lead to further reduction of the runout, since the granular current is only deflected sideways and not launched from the top of the mounds. Thus, the experiments further indicate that mounds can dissipate energy at least as effectively as a continuous dam of the same height, for small heights of the obstacle relative to the flow depth, provided the aspect ratio and mound configuration are chosen carefully. Understanding the formation and geometry of the wedge formed upstream of the mounds is important in the design of mounds for retarding snow avalanches. In particular, the throw angle and thereby the length of the airborne jet depends on the upstream angle of the wedge.

The experiments also suggest certain features in the layout of braking mounds that control their effectiveness. The following conclusions can be drawn about the optimum layout of the mounds:

1. Relative height $H/h \approx 2$. Increasing the height of the mounds relative to the flow thickness beyond $H/h = 2$ does not significantly reduce the runout. Note that snow accumulation on the ground, in the case of real snow-avalanche protection measures, will lead to the need for somewhat higher mounds.

2. The upstream face of the mounds should be steep. For this experimental configuration, an angle $\alpha \approx 60°$ is sufficient since a steeper upstream face only marginally decreases the runout.

3. The proportion of the flow path covered by mounds, $A_{\rm m}/A_{\rm tot}$, should be as large as possible, and the gaps in between the mounds as small and many as possible, with aspect ratios of the mounds maintained at order unity. This is done to obtain maximum mixing of streams in the jet

flow. In some cases, a row of mounds can be more effective than a continuous dam with the same height (Fig. 12).

4. Aspect ratio $H/B \approx 1$. The experiments suggest that having a smaller aspect ratio for the same area covered by the mounds is less effective since some of the material will jump over the mounds and hence not mix with jet streams from neighbouring mounds.

The degree to which the above results apply to natural snow avalanches cannot be determined quantitatively from the small-scale experiments in spite of the Froude numbers being similar in both cases. The formation of wedges at the upstream faces of the mounds for natural avalanches may be expected to depend on the material properties of the snow. As a consequence, the values of H/h, α and H/B suggested above might be different for natural avalanches. The experiments nevertheless provide useful indications for designers of retarding structures for avalanches in the absence of data from experiments at larger scales.

It is noteworthy that mounds may have certain advantages compared to a dam for real snow-avalanche protection measures, with regard to drift-snow accumulation close to the structures.

Experiments at different scales are an interesting subject for future research. Such experiments are needed in order to study whether the experiments scale with the Froude number of the flow, as has been observed for hydraulic energy dissipators. Scaling up the experiments is an obvious next step to take, possibly using snow as the experimental material. In addition to providing information on the energy dissipation at a larger scale, it could also provide direct measurements of the effect of air resistance on the jet. Scaling the experiments down is also of interest. Scale invariance of the flow at the same Froude number at several different laboratory scales would provide a strong indication that results obtained in the laboratory would also apply to natural snow avalanches.

ACKNOWLEDGEMENTS

REFERENCES

Chu, T., G. Hill, D. M. McClung, R. Ngun and R. Sherkat. 1995. Experiments on granular flows to predict avalanche runup. *Can. Geotech. J.*, **32**(2), 285–295.

Gerodetti, M. 1985. Drag coefficient on pyramidal baffle blocks. *Water Power & Dam Construction*, **37**, 26–28.

Hager, W. H. 1995. *Energy dissipators*. Rotterdam, A.A. Balkema.

Hákonardóttir, K.M. 2000. Retarding effects of breaking mounds. Avalanches. (M.Sc. thesis, University of Bristol.)

Hutter, K., T. Koch, C. Plüss and S. B. Savage. 1995. The dynamics of avalanches of granular materials from initiation to runout: Part II. Laboratory experiments. *Acta Mech.*, **109**, 127–165.

Johnson, P. C., P. Nott and R. Jackson. 1990. Frictional–collisional equations of motion for particulate flows and their application to chutes. *J. Fluid Mech.*, **210**, 501–535.

McClung, D. M. and P. A. Schaerer. 1993. *The avalanche handbook*. Seattle, WA, The Mountaineers.

Norem, H. 1994. *Snow engineering for roads*. Oslo, Norwegian Public Administration.

Novak, P., A. I. B. Moffat, C. Nalluri and R. Narayanan. 1989. *Hydraulic structures*. London, Unwin Hyman Ltd.

Peterka, A. J. 1984. *Hydraulic design of stilling basins and energy dissipators*. Denver, CO, U.S. Department of the Interior. U.S. Bureau of Reclamation. (Engineering Monograph 25.)

Roberson, J. A., J. J. Cassidy and M. H. Chaudhry. 1997. *Hydraulic engineering*. Boston, etc., Houghton Mifflin Company.

Salm, B. 1987. *Schnee, Lawinen und Lawinenschutz*. Zürich, Eidgenössische Technische Hochschule Zürich. (Vorlesungsskript.)

Savage, S. B. and K. Hutter. 1989. The motion of a finite mass of granular material down a rough incline. *J. Fluid Mech.*, **199**, 177–215.

Tai, Y. C., J. M. N. T. Gray, K. Hutter and S. Noelle. 2001. Flow of dense avalanches past obstructions. *Ann. Glaciol.*, **32**, 281–284.

Tõmasson, G. G., F. Sigurðsson and F. Rapin. 1998a. The avalanche situation in Neskaupstaður, Iceland. A preliminary defensive plan. *In* Hestnes, E., ed. *25 Years of Snow Avalanche Research, Voss 12–16 May 1998. Proceedings*. Oslo, Norwegian Geotechnical Institute, 283–287. (NGI Publication 203.)

Tõmasson, G. G., F. Sigurðsson and F. Rapin. 1998b. *Neskaupstaður. Avalanche defence appraisal. Drangagil area*. Reykjavík, VST Consulting Engineers. (Report 97.202.)

U.S. Bureau of Reclamation (USBR). 1987. *Design of small dams. Third edition*. Washington, DC, U.S. Department of the Interior. U.S. Bureau of Reclamation.

Voellmy, A. 1955. Über die Zerstörungskraft von Lawinen. *Schweizerische Bauzeitung*, **73**(12/15/17/19), 159–162, 212–217, 246–249, 280–285. (U.S. Department of Agriculture. Forest Service. Alta Avalanche Study Center. Translation 2, 1964.)

Wieland, M., J. M. N. T. Gray and K. Hutter. 1999. Channelized free-surface flow of cohesionless granular avalanches in a chute with shallow lateral curvature. *J. Fluid Mech.*, **392**, 73–100.

Woods, A. W. and A. J. Hogg. 1998. *Snow avalanches. Models of particle-laden currents and avalanche protection measures*. Bristol, University of Bristol. Centre for Environmental and Geophysical Research. School of Mathematics.

Woods, A. W. and A. J. Hogg. 1999. *Experiments on granular flows passing over obstacles on an inclined chute*. Bristol, University of Bristol. Centre for Environmental and Geophysical Research. School of Mathematics